

Article

Spatiotemporal Changes of Farming-Pastoral Ecotone in Northern China, 1954–2005: A Case Study in Zhenlai County, Jilin Province

Yuanyuan Yang ^{1,2,3}, Shuwen Zhang ^{1,2,*}, Dongyan Wang ¹, Jiuchun Yang ² and Xiaoshi Xing ³

¹ College of Earth Science, Jilin University, 2199 Jianshe Street, Changchun 130061, China; E-Mails: sophiayangyuanyuan@hotmail.com (Y.Y.); wang_dy@jlu.edu.cn (D.W.)

² Northeast Institute of Geography and Agroecology, Chinese Academy Sciences, 4888 Shengbei Street, Changchun 130102, China; E-Mail: yangjiuchun0830@163.com

³ Center for International Earth Science Information Network (CIESIN), Earth Institute, Columbia University, P.O. Box 1000 (61 Route 9W), Palisades, NY 10964, USA; E-Mail: xxiaoshi@ciesin.columbia.edu

* Author to whom correspondence should be addressed; E-Mail: zhangshuwen@neigae.ac.cn; Tel.: +86-431-8554-2246.

Academic Editor: Vincenzo Torretta

Received: 3 June 2014 / Accepted: 12 December 2014 / Published: 23 December 2014

Abstract: Analyzing spatiotemporal changes in land use and land cover could provide basic information for appropriate decision-making and thereby plays an essential role in promoting the sustainable use of land resources, especially in ecologically fragile regions. In this paper, a case study was taken in Zhenlai County, which is a part of the farming-pastoral ecotone of Northern China. This study integrated methods of bitemporal change detection and temporal trajectory analysis to trace the paths of land cover change for every location in the study area from 1954 to 2005, using published land cover data based on topographic and environmental background maps and also remotely sensed images including Landsat MSS (Multispectral Scanner) and TM (Thematic Mapper). Meanwhile, the Lorenz curve and Gini coefficient derived from economic models were also used to study the land use structure changes to gain a better understanding of human impact on this fragile ecosystem. Results of bitemporal change detection showed that the most common land cover transition in the study area was an expansion of arable land at the expense of grassland and wetland. Plenty of grassland was converted to other unused land, indicating serious environmental degradation in Zhenlai County during the past decades. Trajectory analysis of land use and land cover change

demonstrated that settlement, arable land, and water bodies were relatively stable in terms of coverage and spatial distribution, while grassland, wetland, and forest land had weak stability. Natural forces were still dominating the environmental processes of the study area, while human-induced changes also played an important role in environmental change. In addition, different types of land use displayed different concentration trends and had large changes during the study period. Arable land was the most decentralized, whereas forest land was the most concentrated. The above results not only revealed notable spatiotemporal features of land use and land cover change in the time series, but also confirmed the applicability and effectiveness of the methodology in our research, which combined bitemporal change detection, temporal trajectory analysis, and a Lorenz curve/Gini coefficient in analyzing spatiotemporal changes in land use and land cover.

Keywords: spatiotemporal changes; land use and land cover change; land use structure; sustainable use of land resources; farming-pastoral ecotone; northern China

1. Introduction

Decadal to centennial land use and land cover change (LUCC) has been widely singled out as an integral component and important driver of global environmental change [1–4]. LUCC could significantly affect key aspects of earth system functioning [5], playing an essential role in moving towards global sustainability. A better understanding and quantification of past spatiotemporal characteristics of land cover change as a fundamental ecological process is important in predicting the development of future land use change and also in informing policy decisions on sustainable use of land resource [6,7].

The farming-pastoral ecotone of Northern China is a sensitive region of terrestrial ecosystems and is very vulnerable to global change and human disturbance. High-intensity human activities have produced enormous negative environmental impacts in the region and the destruction of natural vegetation has constantly drained the service functions of the local ecosystem service [8,9]. This ecotone is alarmingly comparable to the Sahara region in northern Africa [10]. Zhenlai County, as a part of the farming-pastoral ecotone of Northern China, is located in northwestern Jilin province, where the eco-environment is very fragile and is vulnerable to disturbance from various factors. This area was widely covered by grassland before the 1950s, when its eco-environment was relatively stable. After the People's Republic of China was formally established in 1949, soil salinization and grassland degradation became increasingly severe owing to rapid population growth, excessive exploitation, and unreasonable land utilization [11]. Land use structure in the study area has also undergone major changes. Arable, saline, and alkaline lands increased significantly while grassland declined sharply [12–15]. Thus, the sustainable development of the local socio-economy was greatly influenced. It is reported that the irrational land use structure has led to low and unstable yields of arable land, and the severe land degradation has meant people in some towns have poor living conditions [16]. In this context, the study of spatiotemporal changes and land use structure changes over the past decades in Zhenlai County has become a significant topic.

Previous studies of spatiotemporal changes mainly focused on analyzing the categorical changes of land cover with the accumulation of remotely sensed images using a bitemporal detection method [17–20]. The method in those studies analyzed land use and land cover change based on a two-epoch timescale. In general, its application often requires measurements of the area's ratio changes [21,22], the conversion matrix of land cover change [23,24], and the spatial pattern changes characterized by land cover metrics changes [25,26]. To study the human impact on the natural environment, it is often required to recover the history of land cover change and to relate the spatiotemporal pattern of such change with other environmental and human factors [27,28]. Rather than merely relying on the change of areas or other indices, it is also important to effectively analyze the trends of land use and land cover change over time, and to make clear the relationships between the factors that shape the changing nature of human–environment dynamics and their effects within a particular region [28,29]. Trajectory analysis is a method of studying and discovering trends in land cover change in the time series. Attempts have been made to apply a trajectory analysis method on land use and land cover change in multiple time nodes [27–33]. Integrating bitemporal change detection and temporal trajectory analysis could trace the paths of land cover change for every location in an area.

In addition, land use structure could reflect the geographic configuration and comparison of land use types. Analysis of land use structure could provide a better understanding of the relationship between land use and the population–environment system, and also make clear the regional differences and rationality of certain land use structures [34]. The Lorenz curve was an idea originally from economics but has also been applied in many fields by using variables in relevant percentages for intuitive distribution analysis. The Lorenz curve and associated Gini coefficient are simpler compared with current study methods on land use structure, such as the artificial neural network (ANN) [35,36], information entropy [37], optimal linear programming methods [38], and so on. The Lorenz curve and Gini coefficient derived from economic models not only reveal the regularity of change in land use structure and quantify the change process itself, but may also provide approaches for studying the eco–environment [15,39,40].

Satellite images have been used extensively to study temporal changes in land use and land cover in inaccessible areas of China where ground-truth data is lacking [17,18]. However, remotely-sensed data have only existed for the last four decades at most, following the advent of the first land satellite, LandSat-1, launched in 1972. Thus, most researchers could only do related studies in the past 30 years due to the limits on available data. Understanding long-term human–environment interactions is essential to understanding changes in terrestrial ecosystems [41,42]. Thus, it is necessary to study longer-term spatiotemporal changes. This study seeks to use multitemporal satellite images and other data from various sources to analyze spatiotemporal changes in Zhenlai County from 1954 to 2005. Our main objectives are (1) to detect and to evaluate spatiotemporal changes in land use and land cover from 1954 to 2005 in the study area; (2) to trace the paths and to explore the trajectory of land cover change for every location by integrating methods of bitemporal change detection and temporal trajectory analysis; and (3) to analyze the regularity in land use structural changes and to gain a better understanding of human impact on this fragile ecosystem by using the spatial Lorenz curve/Gini coefficient method.

2. Material and Methods

2.1. Study Area

Zhenlai County (N45°28'–N46°18', E122°47'–E124°04') (Figure 1), as a farming-pastoral ecotone, is located in northwestern Jilin province, Northeast China, occupying the northernmost part of the province and bordering Heilongjiang to the east and Inner Mongolia to the west. It is under the administration of Baicheng City. The region was the nomadic land for Mongol princes, and inhabitants were not allowed to reclaim it until the enactment of a “lifting a ban on reclaiming” policy in the late Qing Dynasty (1902). The County boasts a variety of geomorphologic types and features a terrain that is high in the northwest and low in the southeast. Its northwest is adjacent to the Greater Hinggan Mountains, its central area is mostly rolling hilly land, and its east and south surround the Nenjiang River and the Tao'er River, respectively, forming a fertile flood plain on the banks of both rivers. The major soil types are chernozem, alluvium soil, alkali soil, and meadow soil [43].

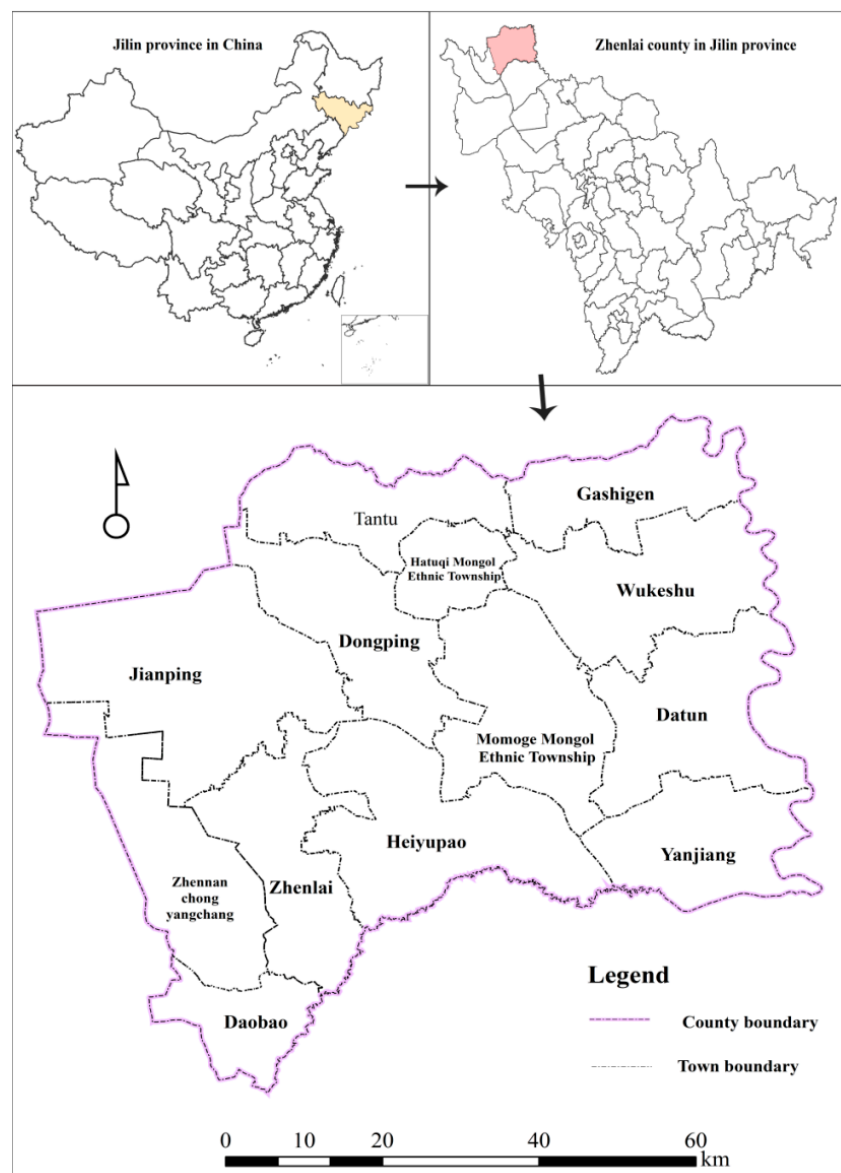


Figure 1. Location of the study area, Zhenlai County.

Climatically, the region is subject to a temperate continental monsoon climate with distinct seasons, as it is located in inland areas of mid-latitude. The mean annual rainfall is 402.4 mm, unevenly distributed over time, while the mean annual evaporation is 1755.9 mm, about four times as high as the mean annual rainfall. Thus, the low amount of precipitation and the high amount of evaporation mainly result in a drought-prone climate in the study area, especially in spring. The mean annual temperature is around 4.9 °C [43].

2.2. Data

Based on our former study about the LUCC rate and the available data in the study area, monitoring of land use and land cover changes was done at four time nodes: 1954, 1976, 2000, and 2005. One Landsat MSS (Multispectral Scanner) and two Landsat TM (Thematic Mapper) images were selected pertaining to the years 1976, 2000, and 2005. Meanwhile, our research team reconstructed the spatiotemporal distribution of land use and land cover in 1954 by making use of topographic maps and physical environmental background maps including those of terrain, climate, geology, soil, vegetation, hydrology, and socioeconomic statistical data. The digital reconstruction model of land use was built based on the cellular automata (CA) model. It consists of five modules: spatial analysis module, sensitivity analysis module, diagnostic module for arable land distribution, demand analysis module, and spatial layout module [44,45].

2.3. Classification System

For comparisons over time, the maps had to be thematically generalized. Taking into account both the local characteristics and the predominant land use classification system used in China [46], the available land classes were aggregated into seven suitable land categories for this study: arable land (including paddy fields and rainfed cropland); forest land (including deciduous forest, coniferous forest, low pinewood, orchards, *etc.*); grassland (including natural grassland and pasture); water bodies (including rivers, lakes, and ponds); settlement (urban and rural construction); wetland; and other unused land (including sand, saline-alkali land, and bare land).

2.4. Methods

2.4.1. Transition Probabilities Matrix for Land Use/Land Cover Dynamics

Within the region of interest we assume a spatially homogeneous probability of transition from one land class to another between time t and time $t+1$. Denote the area of land which switches from class i to class j between time t and $t+1$ by ΔS_{ij}^t , and the area of land in class i at time t by S_i^t . Then the probability of transition from land class i to land class j by P_{ij}^t is estimated as the ratio of these two quantities as follows:

$$P_{ij}^t = \Delta S_{ij}^t / S_i^t \quad (1)$$

However, the above transition probability for land use cannot allow us to fully understand land use change as land use change among various land cover types often has the inverse transition during

different time intervals. In this situation, the concept of cumulative transition probability for land use [47,48] is proposed as in Formula (2):

$$P_{ij} = \left(\sum_{t=1}^n S_{ij}^t / S_T \right) \times 100\% \quad (2)$$

where P_{ij} is the cumulative transition probability for land use from category i to j during the entire study period; i and j are the land use types; S_{ij}^t is the conversion area from category i to j during the time interval t and $t+1$; n is the number of time intervals; and S_T is the total of the study area.

2.4.2. Trajectory Computing Method

Change trajectory of the time series can be expressed by trajectory codes in the form of figures or letters for every parcel in the vector layer [28,30,33]. The numeric code could be operated and calculated in the software ArcGIS, while the letter codes could be used clearly to identify the land use type in the trajectory analysis. Thus, we firstly used the numeric codes to calculate the trajectory of land use change in ArcGIS, and then used the letter codes to analyze the change trajectory. In this study, the following figures were used to stand for each land category for each layer of time node in the trajectory analysis: “1” stands for “Arable land”; “2” stands for “Forest land”; “3” stands for “Grassland”; “4” stands for “Water”; “5” stands for “Settlement”; “6” stands for “Wetland”; and “7” stands for “Other unused land”. Trajectory codes for each parcel can be obtained using Formula (3) as below:

$$Y_i = (G1)_i \times 10^{n-1} + (G2)_i \times 10^{n-2} \dots + (Gn)_i \times 10^{n-n} \quad (3)$$

where Y_i is the trajectory code of the parcel i in the trajectory layer; n is the number of time nodes; and $(G1)_i$, $(G2)_i$, and $(Gn)_i$ are the codes of the land use/cover type of each time node at the given parcel.

Thus, the trajectory codes (e.g., 3631, 1333) of every parcel can be calculated automatically. Then, we used the following letter codes to replace the numeric codes: “A” stands for “Arable land”; “F” stands for “Forest land”; “G” stands for “Grassland”; “W” stands for “Water”; “S” stands for “Settlement”; “M” stands for “Wetland”; and “O” stands for “Other unused land”. In addition, we used the symbol “→” to show the change direction in time series. Thus, the above trajectory codes “3631” would be replaced by “G→M→G→A”, which means that the land was found to be grassland in 1954, wetland in 1956, grassland again in 2000, and cultivated as arable land in 2005; “1333” would be replaced by “A→G→G→G”, which means that the land was found to be arable land in 1954 and abandoned as grassland in 1976, 2000, and 2005. Not only can the land use/cover change for every parcel and every time node in the study area be shown in the trajectory codes, but also the trajectory for every parcel through the time series can be specified by land categories (Figure 2).

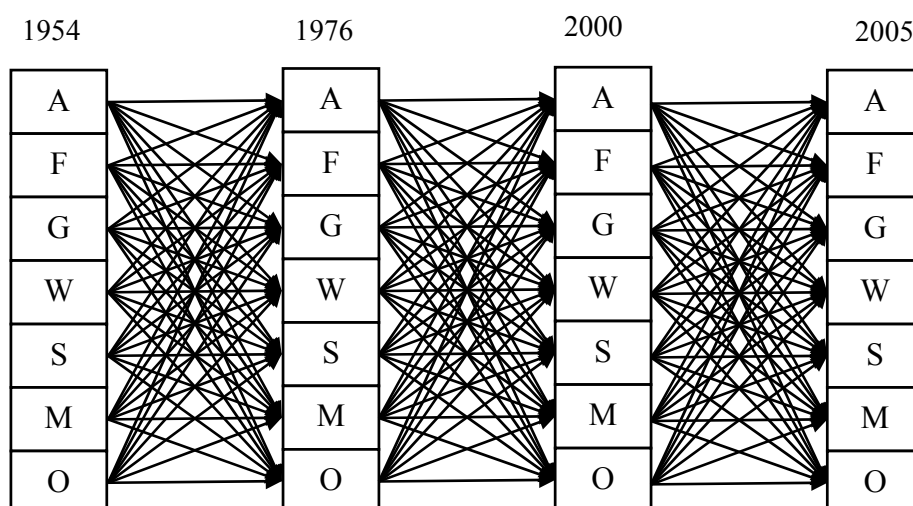


Figure 2. All the possible trajectories of the land use/cover change in the study period.

2.4.3. Establishing the Trajectories of Land Use

We classified all the trajectories of land cover change into four generic classes—unchanged land cover, and one-step, two-step, and three-step changed land cover—according to the numbers of change. The unchanged class refers to the land cover that stays the same during the study period, such as “G→G→G→G” which means that the land cover type was grassland and remained the same through the given four time nodes. One-step changed land cover includes trajectories such as “A→G→G→G”, “A→A→G→G” and “A→A→A→G”, indicating that there is only one land change no matter when it happened over the study period. Similarly, two-step changed land refers to land that changes twice from 1954 to 2005, such as “G→A→G→G” or “G→G→A→G”. Three-step changed land (e.g., A→G→F→A) often has the smallest probability of happening. Analyzing the four generic classes will indicate the frequency of land change in the study area and analysis of the underlying sequence of changes will reveal when the land change happened. For example, “G→A→A→A” shows that people reclaimed land during 1954–1976, and “G→G→A→S” indicates that land was cultivated between 1976 and 2000 and then arable land converted to settlements during the period from 2000 to 2005.

From another perspective, land changes were also classified into three generic classes, namely, unchanged, human-induced, and natural evolution-induced changes based on human impact on the environment [27]. Human-induced change means a process where land ecosystem changes into an artificial one in the form of sudden change affected directly by human activities, such as grassland→arable land. Natural evolution-induced types, including changes due to natural processes (e.g., land desertification and soil salinization) or minor/indirect human activities, are often in the form of gradual change. According to Table 1, we can distinguish the human-induced type from the natural evolution-induced type for one-step changed land cover. As for two-step or three-step changed land cover, we define them as human-induced as long as at least one of the observed land-use changes is the human-induced type as defined in Table 1, no matter when it happens. For example, “M→G→G→A”, “A→F→A→A”, and “A→G→F→A” are defined as human-induced types while “W→M→G→O” and “G→W→M→G” are natural evolution-induced types.

Table 1. Land-use change types.

Human-induced type				Natural evolution-induced type			
A→F	A→G	A→S	F→A	A→W	A→M	A→O	G→W
F→G	F→S	G→A	G→F	G→M	G→O	W→G	W→M
G→S	W→A	W→F	W→S	W→O	M→G	M→W	M→O
M→A	M→F	M→S	O→F	O→G	O→W	O→M	

2.4.4. Spatial Lorenz Curve and Gini Coefficient

In this study we developed a Lorenz curve and Gini coefficient describing the spatial aggregation of each of the seven land use types by dividing Zhenlai County into distinct areas associated with different towns. The procedure used for drawing spatial Lorenz curves involved three steps. Firstly, each town's location entropy was calculated according to the data of land-use area in the years 1954, 1976, 2000, and 2005. Location entropy is known as specialized rate and is calculated by Formula (4):

$$Q = (A1 / A2) / (B1 / B2) \quad (4)$$

where Q is location entropy; $A1$ is the area of a certain type of land use in a town; $A2$ is the total area of a certain type of land use in Zhenlai County; $B1$ is the total area of the same town; and $B2$ is the total area of Zhenlai County.

Secondly, according to the magnitude of the location entropy for each town and land use, the location entropy of each town was sorted from small to large and then the cumulative percentages of each town's area to the total land area were calculated. Thirdly, the spatial Lorenz curves were plotted. The X-coordinate represents the accumulated percentage of a total land area and Y-coordinate stands for the accumulated percentage of the type of land use. A straight line with no bending corresponds to the perfect equality line and the curve bends indicate the concentration degree of land use spatial distribution in the study area.

By quantifying the bends of the spatial Lorenz curve, the Gini coefficient is calculated by Formula (5):

$$G = \sum_{i=1}^{n-1} (M_i Q_{i+1} - M_{i+1} Q_i) \quad (5)$$

where G is the Gini coefficient; M_i is the accumulated percentage of a given type of land use in a given town; Q_i is the accumulated percentage of each town's land area to the total land area; n is the number of towns in the study area; and $i = 1 - n$. In this paper, the study area includes 13 towns, so the value range of the integer i is $0 < i < 14$. According to the commonly used division standard of the Gini coefficient, the distribution characteristics of land use can be estimated as follows: when $0 < G \leq 0.2$ stands for absolute decentralization; $0.2 < G \leq 0.3$ represents decentralization; $0.3 < G \leq 0.4$ indicates appropriate concentration; $0.4 < G \leq 0.5$ means concentration; and $0.5 < G \leq 1$ corresponds to absolute concentration [15].

3. Results and Discussion

3.1. Land Use and Land Cover Change (1954–2005)

3.1.1. Temporal Properties

It was found that the land use/cover changed significantly after statistical analysis of the land-use area over the study period in Zhenlai County (Table 2 and Figure 3). In 1954–2005, arable land, grassland, and wetland were the dominant land use types, with over 70% of total area percentage. Arable land, forest, and settlement expanded continuously from 1954 to 2005 (Figure 4). It is especially important to note that arable land had the largest increase, from 31.48% in 1954 to 39.07% in 2005, while both grassland and wetland had significant loss during the past 60 years. In 1954, grassland and wetland occupied 30.54% and 32.26% of the total study area; however, these areas had declined to 12.27% and 18.81%, respectively, by 2005. The proportional area of water bodies changed slightly, fluctuating from 4.89% in 1954 to 5.50% in 2005. Water bodies were mainly influenced by natural factors, especially affected by climate change in the absence of irrigation facilities such as reservoirs. Other unused land surged from 1954 to 1976 and continued to increase until 2000, and then it began to decline slightly as people started to emphasize controlling desertification and salinization.

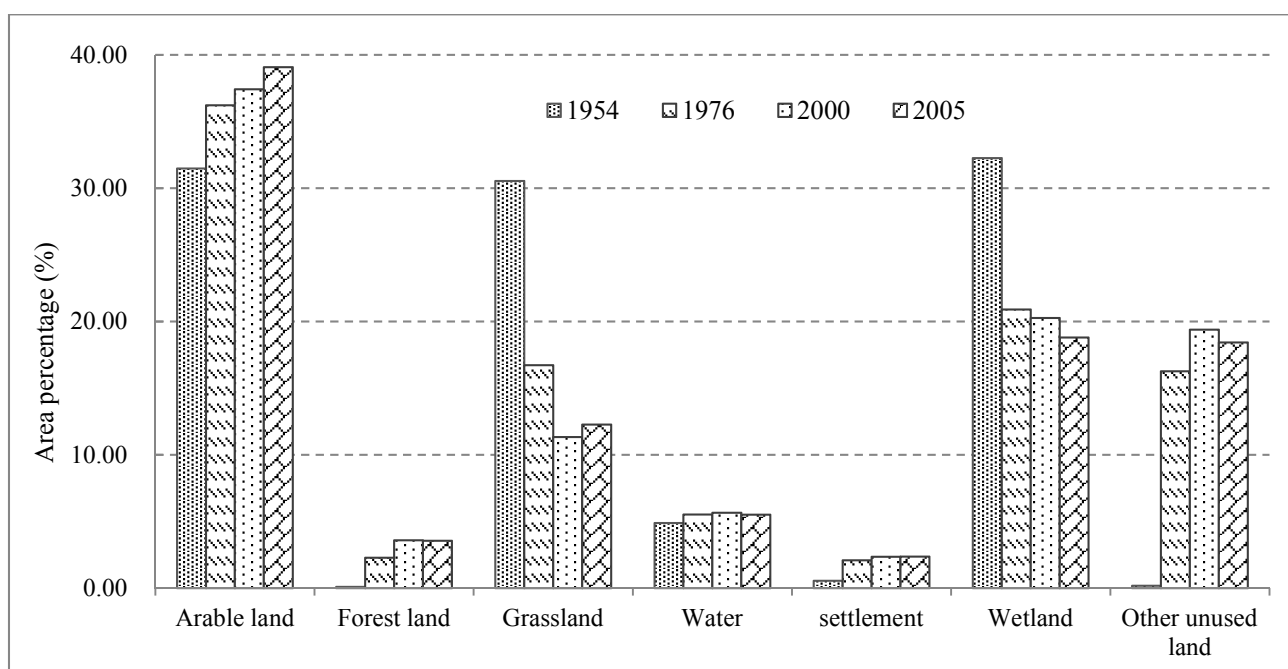
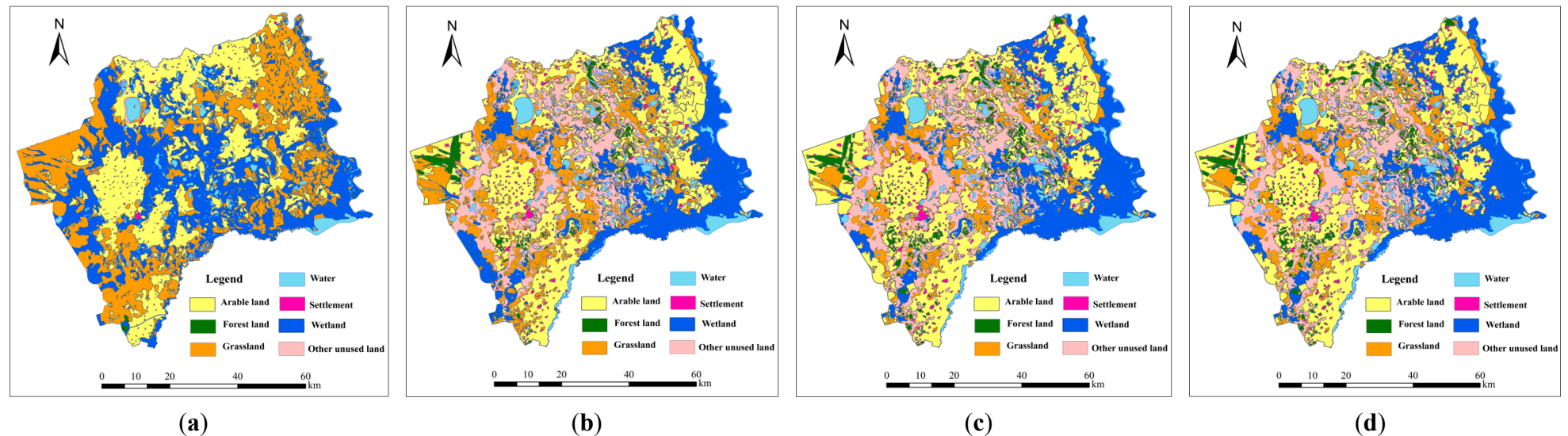


Figure 3. Percentage of area of each land category, 1954–2005.

Table 2. Area and percentage changes during the time intervals.

Categories	Area (in ha) and percentages (%)								Changes (in ha)		
	1954		1976		2000		2005		1954–1976	1976–2000	2000–2005
	Area	%	Area	%	Area	%	Area	%			
Arable land	16,7355.69	31.48	19,2533.35	36.22	198,950.45	37.42	207,717.83	39.07	25,177.66	6417.10	8767.38
Forest land	488.65	0.09	12,117.17	2.28	19,065.53	3.59	18,900.88	3.56	11,628.51	6948.36	−164.65
Grassland	16,2371.84	30.54	88,892.09	16.72	60,215.14	11.33	65,223.77	12.27	−73,479.75	−28,676.94	5008.63
Water	26,000.01	4.89	29,352.35	5.52	30,024.12	5.65	29,259.09	5.50	3352.34	671.78	−765.03
Settlement	2944.58	0.55	11,109.70	2.09	12,503.21	2.35	12,547.33	2.36	8165.12	1393.51	44.12
Wetland	17,1500.15	32.26	111,101.27	20.90	107,753.65	20.27	99,975.96	18.81	−60,398.88	−3347.62	−7777.69
Other unused land	945.22	0.18	86,500.22	16.27	103,094.04	19.39	97,981.28	18.43	85,555.01	16,593.82	−5112.76

**Figure 4.** Land use/cover maps for the years (a) 1954; (b) 1976; (c) 2000 and (d) 2005.

3.1.2. Bitemporal Change Detection

A transition matrix was used to summarize the state of each land use in each time interval and the transitions through time with respect to each land category. From Tables 3 and 4, and Figure 5, the results indicated that arable land expanded at the expense of grassland and wetland. Grassland had the largest cumulative transition probability (34.37%) during the period from 1954 to 2005, and 15.41% of grassland was changed into arable land while 15.02% of grassland was converted to wetland and other unused land. However, from 1954 to 1976, 38.90% of grassland was turned into arable land due to the fast growth of the population (from 145,328 persons in 1954 to 277,146 persons in 1976). Furthermore, 24.20% of grassland was converted to other unused land during 1976–2000, indicating serious environmental degradation. Wetland had the second largest cumulative transition probability (32.90%) during the study period. Wetland was mainly changed into arable land and other unused land, reflecting both human activities and natural processes affected by the climate. Wetland was changed to arable land with similar transition probabilities during the three time intervals from 1954 to 1976 (11.79%), 1976 to 2000 (16.75%), and 2000 to 2005 (15.45%). Also, 33.35% of wetland was changed to other unused land between 1954 and 1976. In addition, abandoned land could not be ignored during the study area. The cumulative transition probability of arable land is 26.20%, ranking third.

Table 3. Transition probability matrices of land changes in each period (%).

Categories	Period	Arable land	Forest land	Grassland	Water	Settlement	Wetland	Other unused land
Arable land	1954–1976	56.19	3.74	15.58	2.01	5.55	8.51	8.42
	1976–2000	81.27	1.80	2.91	0.10	2.84	11.05	0.04
	2000–2005	84.97	5.87	0.00	0.00	9.16	0.00	0.00
Forest land	1954–1976	12.99	21.04	57.91	0.00	5.26	2.81	0.00
	1976–2000	19.93	79.80	0.00	0.00	0.26	0.00	0.00
	2000–2005	15.86	84.14	0.00	0.00	0.00	0.00	0.00
Grassland	1954–1976	38.90	3.96	18.28	2.25	1.15	24.55	10.90
	1976–2000	10.11	9.83	54.66	0.23	0.13	0.84	24.20
	2000–2005	16.19	0.00	83.81	0.00	0.00	0.00	0.00
Water	1954–1976	5.89	0.19	4.78	41.97	0.14	25.16	21.87
	1976–2000	2.50	2.50	2.50	85.00	2.50	2.50	2.50
	2000–2005	1.39	0.00	3.15	70.41	0.00	23.33	1.72
Settlement	1954–1976	36.31	0.79	5.91	0.82	42.04	3.76	10.37
	1976–2000	2.50	2.50	2.50	2.50	85.00	2.50	2.50
	2000–2005	2.50	2.50	2.50	2.50	85.00	2.50	2.50
Wetland	1954–1976	11.79	0.58	20.15	6.02	0.41	27.70	33.35
	1976–2000	16.75	0.00	4.05	0.83	0.00	77.86	0.52
	2000–2005	15.45	0.00	0.25	8.68	0.00	75.62	0.00
Other unused land	1954–1976	0.44	0.00	1.14	85.29	0.00	7.53	5.60
	1976–2000	0.69	0.00	0.00	3.20	0.33	11.33	84.44
	2000–2005	0.09	0.00	18.64	0.55	0.00	0.19	80.53

Table 4. Cumulative transition probabilities (%).

1954–2005	Arable land	Forest land	Grassland	Water	Settlement	Wetland	Other unused land	Total
Arable land	0.00	4.03	5.96	0.67	6.20	6.68	2.67	26.20
Forest land	1.04	0.00	0.05	0.00	0.01	0.00	0.00	1.10
Grassland	15.41	2.85	0.00	0.73	0.37	7.64	7.38	34.37
Water	0.50	0.15	0.55	0.00	0.14	2.69	1.30	5.34
Settlement	0.31	0.12	0.14	0.12	0.00	0.13	0.17	0.99
Wetland	10.44	0.19	7.40	3.87	0.13	0.00	10.87	32.90
Other unused land	0.13	0.00	3.62	0.78	0.05	1.89	0.00	6.47

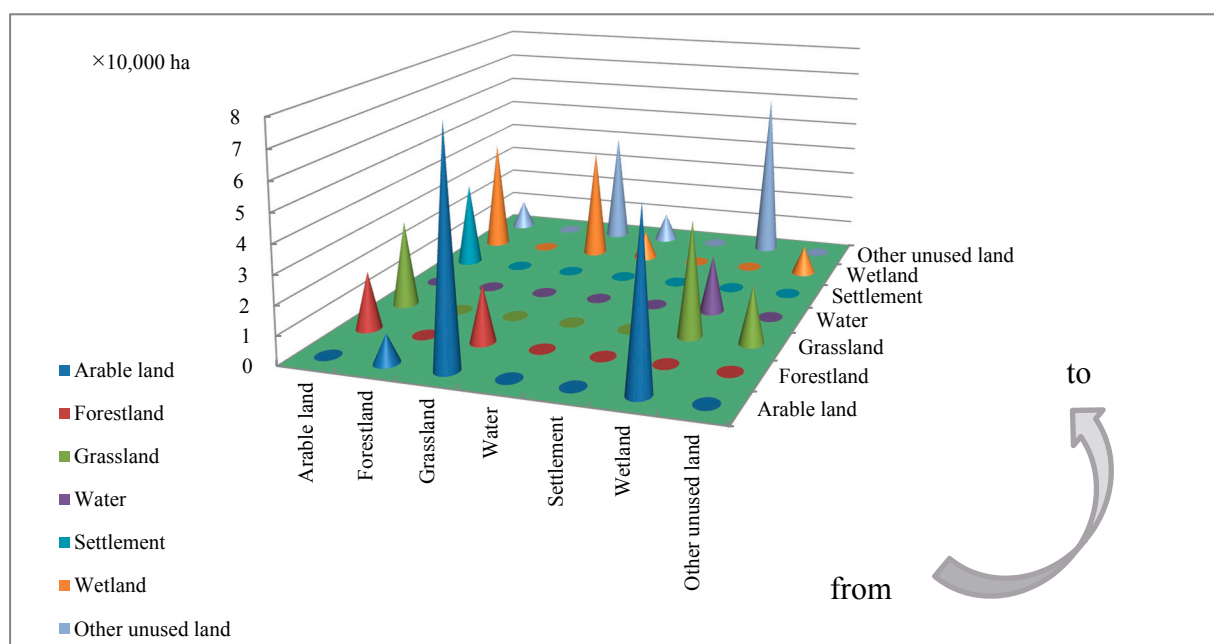


Figure 5. Cumulative transition areas from 1954 to 2005 ($\times 10,000$ ha).

3.1.3. Spatial Distributions and Trajectories of Land Cover Change

During the study period, unchanged land occupied 35.83% of the total area, and one-step, two-step, and three-step changed land occupied 55.54%, 8.07%, and 0.56%, respectively. Taking land use data in 1954 as a baseline, 64.80% of arable land, 49.33% of settlement, and 44.91% of water bodies remained the same during the study period (Table 5), indicating that these land categories had relatively strong stability and certainty in the spatial distributions.

Table 5. Percentages of unchanged land areas to the corresponding land areas in 1954 by types (%): A = Arable land; F = Forest land; G = Grassland; W = Water; S = Settlement; M = Wetland; O = Other unused land.

Unchanged land use	%	Unchanged land use	%	Unchanged land use	%	Unchanged land use	%
A	64.80	F	24.97	G	13.53	W	44.91
S	49.33	M	27.26	O	6.88		

There were 34 types of one-step land changes (Table 6), mainly including grassland→arable land (18.33%), wetland→other unused land (14.95%), grassland→wetland (8.71%), wetland→grassland (6.80%), grassland→other unused land (6.22%), and wetland→arable land (6.17%). The rest of the one-step changes were less than 4%. Moreover, among these one-step changed trajectories, “G→A→A→A” contributed the largest percentage (16.80% of the total changed land area from 1954 to 2005), while “G→G→A→A” and “G→G→G→A” contributed the percentages of 1.50% and 0.03%, respectively. The percentages of “M→A→A→A”, “M→M→A→A” and “M→M→M→A” contributed 4.74%, 0.89%, and 0.54%, respectively. The above analyses illustrated that people reclaimed and cultivated land intensely during 1954–1976, creating the dominant effect on land use. This could be driven by the national macro-policy actively encouraging people to reclaim and farm to develop local agriculture. The adjustment of production relations mobilized people’s enthusiasm to reclaim land since the 1950s [49,50]. One-step changes showed that once one land type was changed to another, it would then reach a steady state. For example, two-step changed land use would not occur if a quantity of grassland was changed into arable land. This might illustrate that people would not easily give up their reclaimed land unless an irresistible force exists. “Wetland→Other unused land” indicated that land degradation has difficult reversibility. Moreover, there were many conversions between grassland and wetland for the following two reasons: (1) wetland had a clear relationship with precipitation and would be changed into grassland in the years with less precipitation; (2) there were plenty of lakes and ponds inside and surrounding the Nenjiang River and the Tao’er River to the east and south of the study area, respectively, which made the nearby wetland, grassland, and other unused land convert frequently.

There were 60 types of two-step changes, mainly including wetland→grassland→other unused land (2.08%), grassland→wetland→arable land (1.93%), and arable land→grassland→forest land (1.43%). However, there were only 13 types of three-step changes, all with small percentages of the areas. Altogether, the analysis of two-step and three-step changes showed that arable land, grassland, wetland, water bodies, and other unused land were converted frequently; this may be due to the influence of rainfall.

Figure 6c shows that the trajectory analysis of land cover can display the histories of land use change and their features related to different driving forces over the study period. During the 60-year study period, unchanged land occupied 35.83% of the total area, human-induced changes occupied 26.89%, and natural evolution land area occupied 37.28%, respectively. In the study area, human-induced changes were mainly distributed in two areas, namely, cultivation in the northwest and east along the Nenjiang River. Unchanged, natural, and human-induced land use appeared stepwise from east (along the Nenjiang River) to west. Natural change along the Nenjiang River was likely to be caused by the fluctuation between flooding and drying. The fertile flood plain on the river’s banks allowed the land to be cultivated easily and produce a high grain yield.

From 1954 to 2005, once unchanged land and the land influenced by natural type were subject to human-induced changes, they tended to reach stability and were less likely to change in the following time nodes. In contrast, areas where changes were once influenced by natural evolution were more likely to change further. A plausible explanation for this is that land cover tends to be changed into a certain type that could increase its value or improve quality due to human activities. If it is converted into another type, the land value tends to decline or the switching cost tends to increase. Thus, it sometimes may drastically reduce the possibility that the land is used for other purposes. Analysis found that grassland,

which decreased—the opposite of the continuously increasing artificial ecological environment construction—was changed into arable land and settlement. Moreover, water bodies, settlement, and arable land, which were closely related to human activities, were the most stable types. The second was other unused land related to land degradation, including sand, saline-alkali land, and bare land, whereas forest land, grassland, and wetland had the weakest stability. It is plausible to suggest that these illustrate the following three phenomena: (1) people do not easily give up their reclaimed land; (2) water bodies were difficult to replace by other land-use types; and (3) land degradation was often irreversible, at least on the observed time scales. Grassland and wetland with greater plasticity tended to be reclaimed into cultivated land and were affected by human impact on land development. In addition, land-use conversions often occur between grassland and wetland, or among wetland, water bodies, saline, and alkaline land influenced by precipitation.

Table 6. Percentages of changed land areas by types, 1954–2005 (%). A = Arable land; F = Forest land; G = Grassland; W = Water; S = Settlement; M = Wetland; O = Other unused land.

	Changed types	%	Changed types	%	Changed types	%	Changed types	%
One-step changes	A→G	3.28	A→S	2.33	A→F	1.55	A→O	3.13
	A→W	0.53	A→M	3.11	G→A	18.33	G→S	0.53
	G→F	2.05	G→O	6.22	G→W	0.84	G→M	8.71
	F→G	0.02	F→A	0.02	F→S	0.01	W→G	0.28
	W→A	0.38	W→S	0.01	W→F	0.01	W→O	1.44
	W→M	1.56	S→G	0.03	S→A	0.25	S→O	0.08
	S→W	0.01	S→M	0.03	M→G	6.80	M→A	6.17
	M→S	0.19	M→F	0.26	M→O	14.95	M→W	3.25
	O→W	0.20	O→M	0.02				
Two-step changes	A→G→A	0.40	A→G→S	0.01	A→G→F	1.43	A→G→O	0.62
	A→G→M	0.03	A→F→A	0.06	A→O→G	0.06	A→O→A	0.01
	A→O→M	0.01	A→W→G	0.02	A→W→M	0.21	A→M→A	0.25
	A→M→W	0.02	G→A→G	0.23	G→A→S	0.08	G→A→F	0.04
	G→A→M	0.48	G→F→A	0.19	G→O→G	0.52	G→O→A	0.01
	G→O→W	0.06	G→W→G	0.01	G→W→M	0.18	G→M→G	0.37
	G→M→A	1.93	G→M→O	0.03	G→M→W	0.16	S→G→O	0.01
	S→A→S	0.02	S→A→F	0.01	F→G→F	0.05	O→W→G	0.03
	W→G→O	0.11	W→G→W	0.01	W→G→M	0.01	W→O→G	0.02
	W→O→W	0.01	W→O→M	0.02	W→M→G	0.01	W→M→A	0.21
	W→M→O	0.01	W→M→W	0.05	M→G→A	0.37	M→G→S	0.01
	M→G→F	0.10	M→G→O	2.08	M→G→W	0.01	M→G→M	0.12
	M→A→G	0.14	M→A→S	0.07	M→A→W	0.01	M→A→M	0.37
	M→F→A	0.02	M→O→G	0.60	M→O→W	0.01	M→O→M	0.10
	M→W→G	0.01	M→W→A	0.03	M→W→O	0.04	M→W→M	0.55
Three-step changes	A→G→O→G	0.20	A→G→W→M	0.01	A→M→W→M	0.01	F→G→O→G	0.01
	G→A→G→A	0.01	G→A→M→A	0.21	G→M→W→M	0.04	W→A→M→A	0.04
	W→G→O→G	0.01	W→M→W→M	0.01	M→A→M→A	0.20	M→G→O→G	0.10
	M→G→W→M	0.03						

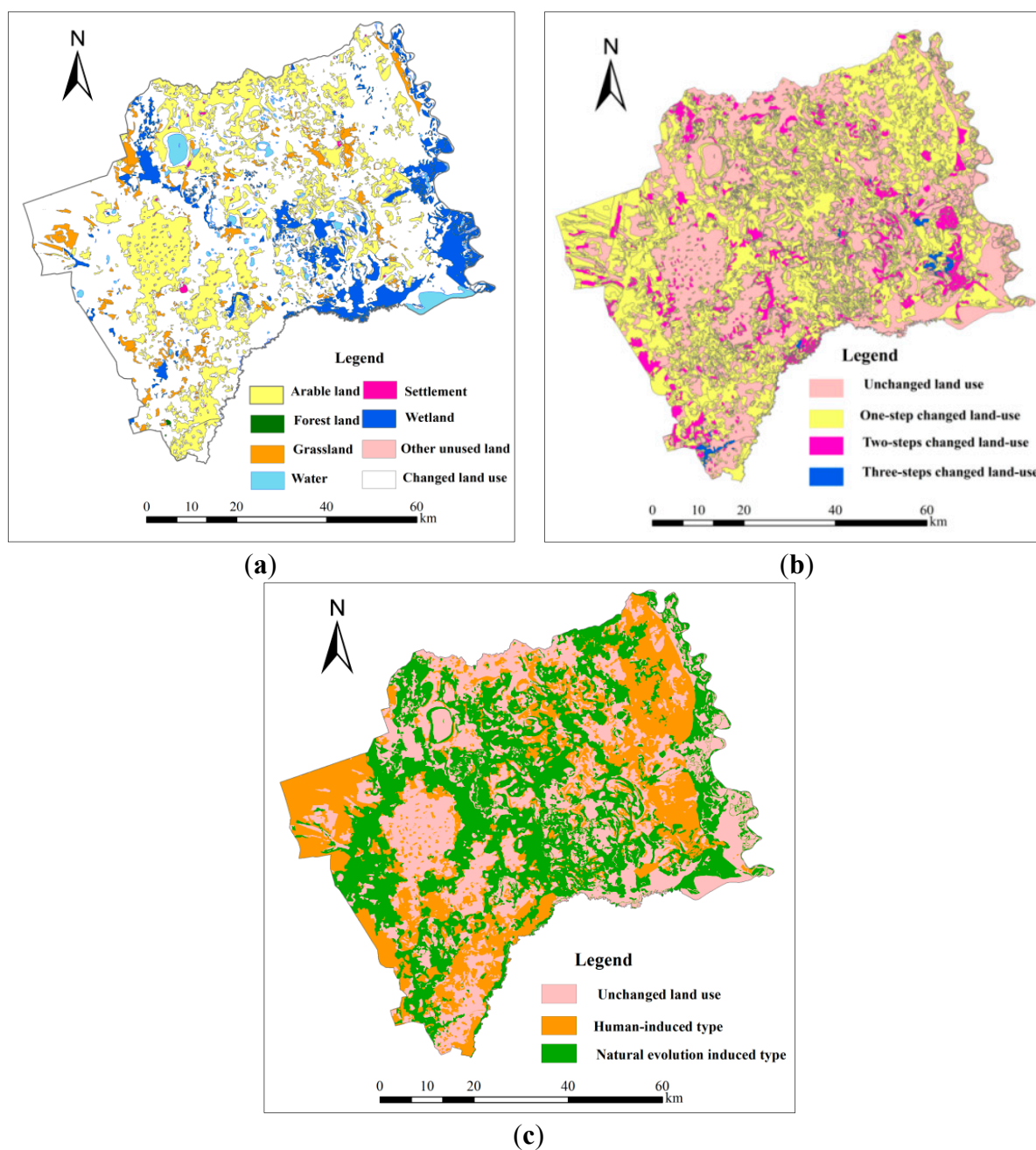


Figure 6. Trajectories of unchanged land use (a) and land use changes (b,c), 1954–2005.

3.2. Land Use Structure

The spatial Lorenz curves for the various land use types are shown in Figure 7. The spatial Lorenz curves of arable land are always the nearest to the perfect equality line in the study period, those of settlement are second, and those of grassland are third. Land curves of forest are always the farthest. These characteristics illustrate that arable land showed the most decentralized distribution among the seven land use types, followed by settlement and grassland. Meanwhile, forest land exhibited the most concentrated distribution, especially in 1954. Water bodies, wetland, and other unused land had different characteristics and showed distinct concentrated distribution at the four time nodes.

Figure 7 qualitatively demonstrates the respective distribution of land use structure between 1954 and 2005, while the Gini coefficient in the study area (Table 7 and Figure 8) quantitatively measures changes

of land use structure in the study period. From 1954 to 2005, there were great changes in the Gini coefficients, especially those for forest land and other unused land. The average Gini coefficient of arable land is 0.2141, the smallest among the Gini coefficients of the seven land use types. The results indicate that during the study period, arable land was decentralized and had a trend of decentralized use explained by the decreasing Gini coefficients over time. The average Gini coefficients of settlement and grassland are 0.2848 and 0.2939, respectively, indicating that these two types of land use were distributed in decentralized manners, with different change trends. Grassland had the minimal fluctuation. Water bodies exhibited appropriate concentration, with an average Gini coefficient of 0.4186, and water bodies tended toward concentration. Forest land had the highest average Gini coefficient at 0.6001, showing absolute concentration. Other unused land had similar characteristics to forest land, and a decreasing trend was clearly observable, especially from 1954 to 1976.

These changes in the Gini coefficients are consistent with the changes of the land use area. The area of arable land and settlement increased during the study period, whereas their corresponding Gini coefficients decreased and the spatial distributions were more even. Increases in cultivated land were consistent with the result of population growth and excessive reclamation of land, which could be reflected by increasing settlement. The growth of other unused land and the decrease of grassland and wetland reflected the deterioration of the eco-environment [15,51] and therefore provided some evidence indicating that the quality of the ecological environment declined year by year over the past decades.

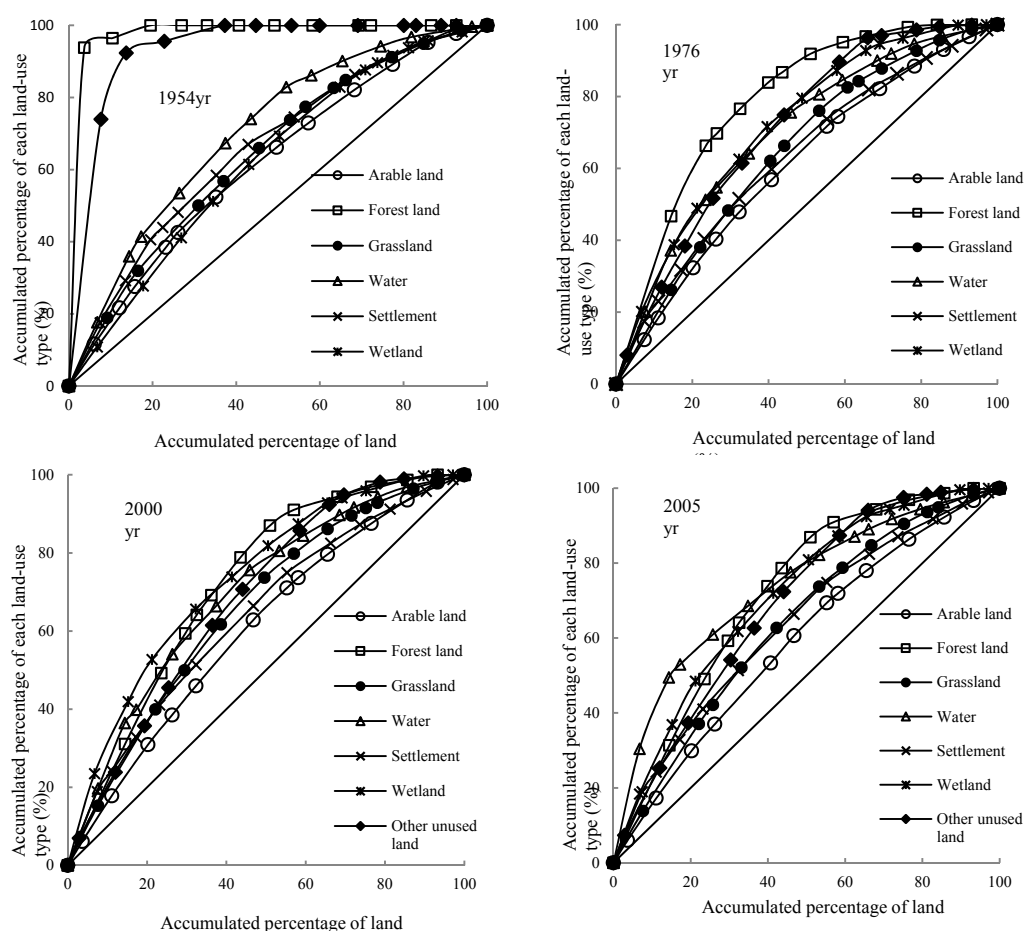


Figure 7. Spatial Lorenz curves of various land use types.

Table 7. Spatial distribution structures and divisions of different land use types.

Year	Arable land	Forest land	Grassland	Water	Settlement	Wetland	Other unused land
1954	0.2407	0.9513	0.2900	0.4121	0.3222	0.2513	0.8661
1976	0.2195	0.5711	0.2964	0.4000	0.2640	0.4395	0.4253
2000	0.2116	0.4394	0.3136	0.3924	0.2770	0.4626	0.3672
2005	0.1845	0.4386	0.2759	0.4700	0.2760	0.4253	0.3872
Average value	0.2141	0.6001	0.2939	0.4186	0.2848	0.3947	0.5115
Distribution division	Decentralization	Absolute concentration	Decentralization	Concentration	Decentralization	Appropriate concentration	Absolute concentration

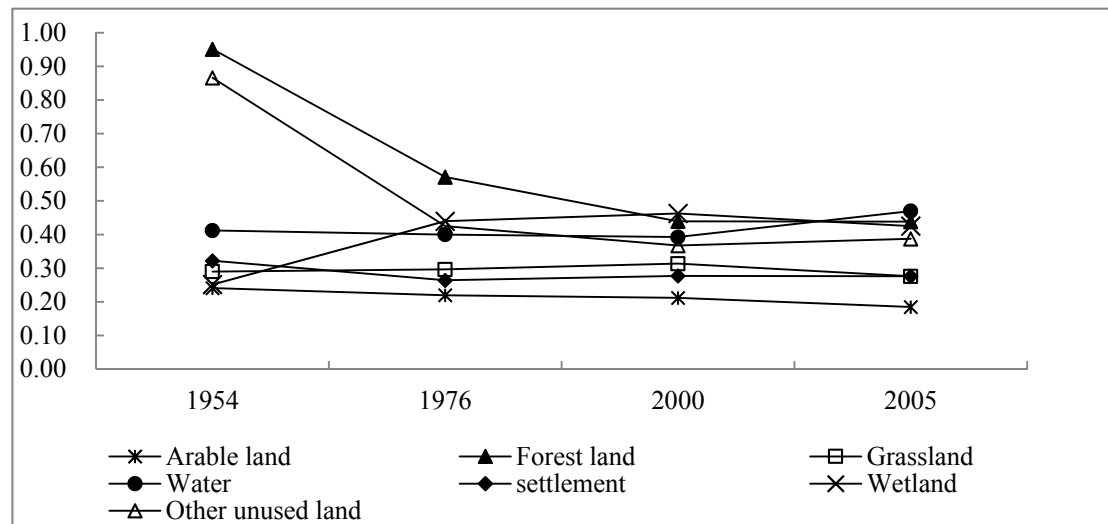


Figure 8. Changes in Gini coefficients of different land use types from 1954 to 2005.

4. Conclusions

In this paper, we used published land cover data, based on topographic and environmental background maps and also remotely sensed images including Landsat MSS and TM, to study the spatiotemporal changes of land use and land cover from 1954 to 2005 in Zhenlai County, Jilin province, northeast China. This study integrated methods of bitemporal change detection and temporal trajectory analysis to trace the paths of land cover change for every location, and to identify the stability of land-use conversion and human-induced environmental change. Spatial distribution structures of different land use types were also analyzed by using the Lorenz curve and associated Gini coefficient. The findings of the case study can be summarized as follows.

- (1) The results of bitemporal change detection showed that land use/cover changed significantly in Zhenlai County from 1954 to 2005. Arable land expanded at the expense of grassland and wetland. Meanwhile, plenty of grassland was converted to other unused land, indicating serious environmental degradation in Zhenlai County during the past decades.
- (2) Trajectory analysis of land use and land cover change demonstrated that settlement, arable land, and water bodies were relatively stable in terms of coverage and spatial distribution, while grassland, wetland, and forest land had weak stability. Many transitions from wetland to other unused land indicated that land degradation had difficult reversibility. Furthermore, human-induced changes, representing an irreversible impact on the environment, could be distinguished from changes caused by natural forces by using this trajectory analysis. The results suggested that natural forces were still dominating the environmental processes of the study area, with unchanged (35.83% of the total area) and indecisive changes between land-cover types (37.28%). However, human-induced changes, constituting 26.89% of the total area, also played an important role in environmental change.
- (3) The research showed that the Lorenz curve/Gini coefficient could be applied effectively to analyze the land use structure changes. The seven types of land use displayed different concentration trends and had large changes during 1954 and 2005. Arable land was the most decentralized, whereas forest land was the most concentrated.
- (4) Previous studies of spatiotemporal changes mainly focused on analyzing the categorical changes of land cover with the accumulation of remotely sensed images using a bitemporal detection method. It assumed spatially homogeneous transition rates and therefore was of limited use in projecting future changes. The above results not only revealed notable spatiotemporal features of land use/cover change in the time series, but also confirmed the applicability and effectiveness of the combined methods of bitemporal change detection, temporal trajectory analysis, and a Lorenz curve/Gini coefficient. Integrating methods of bitemporal change detection and temporal trajectory analysis could explore the trajectories of land cover change by analyzing the extent to which land use conversion is explained by the concept of stability and by distinguishing human-induced land changes from natural evolution types, and then could effectively trace the paths of land cover change for every location. Meanwhile, the Lorenz curve and Gini coefficient of economic models could supplement and reveal the regularity in land use structural changes to gain a better understanding of the human impact on this fragile ecosystem.

Acknowledgments

We thank the three reviewers for their constructive comments and suggestions. This research was funded by the Strategic Priority Research Program of the Chinese Academy of Sciences (No. XDA05090310), the National Natural Science Foundation of China (No. 41271416), and the State Scholarship Fund of China. The paper was also completed with support from the Center for International Earth Science Information Network (CIESIN), Columbia University, USA. We would like to thank Robert S. Chen and Alex de Sherbinin of CIESIN for their valuable suggestions.

Author Contributions

Yuanyuan Yang and Shuwen Zhang conceived and designed the research; Shuwen Zhang and Jiuchun Yang collected and processed the data; Yuanyuan Yang, Dongyan Wang and Xiaoshi Xing analyzed the data. All authors have read and approved the final manuscript.

Conflicts of Interest

The authors declare no conflict of interest.

References

1. Lambin, E.F. Modelling and monitoring land-cover change processes in tropical regions. *Prog. Phys. Geogr.* **1997**, *21*, 375–393.
2. Turner, B.L.; Lambin, E.F.; Reenberg, A. The emergence of land change science for global environmental change and sustainability. *Proc. Natl. Acad. Sci. USA* **2007**, *104*, 20666–20671.
3. Foster, D.; Swanson, F.; Aber, J.; Burke, I.; Brokaw, N.; Tilman, D.; Knapp, A. The importance of land-use legacies to ecology and conservation. *Bioscience* **2003**, *53*, 77–88.
4. Gragson, T.L.; Bolstad, P.V. Land use legacies and the future of southern Appalachia. *Soc. Nat. Resour.* **2006**, *19*, 175–190.
5. Lambin, E.F.; Turner, B.L.; Geist, H.J.; Agbola, S.B.; Angelsen, A.; Bruce, J.W.; Coomesf, O.T.; Dirzog, R.; Fischerh, G.; Folkei, C.; *et al.* The causes of land-use and land-cover change: Moving beyond the myths. *Glob. Environ. Chang.* **2001**, *11*, 261–269.
6. Chauchard, S.; Carcaillet, C.; Guibal, F. Patterns of land-use abandonment control tree-recruitment and forest dynamics in Mediterranean mountains. *Ecosystems* **2007**, *10*, 936–948.
7. DeFries, R.S.; Eshleman, K.N. Land-use change and hydrologic processes: A major focus for the future. *Hydrol. Process.* **2004**, *18*, 2183–2186.
8. Costanza, R.; d’Arge, R.; de Groot, R.; Farber, S.; Grasso, M.; Hannon, B.; Limburg, K.; Naeem, S.; O’Neill, R.V.; Paruelo, J.; *et al.* The value of the world’s ecosystem service and natural capital. *Nature* **1997**, *387*, 253–260.
9. Chen, Y.H.; Li, X.B.; Su, W.; Li, Y. Simulating the optimal land-use pattern in the farming-pastoral transitional zone of Northern China. *Computers. Environ. Urban Syst.* **2008**, *32*, 407–414.
10. Wang, J.A.; Xu, X.; Liu, P.F. Land use and carrying capacity in ecotone between agriculture and animal husbandry in northern China. *Resour. Sci.* **1999**, *21*, 19–24. (In Chinese)

11. Lin, N.; Tang, J.; Bian, J.M.; Yang, J.Q. The quaternary environmental evolution and the problem of desertification in northeast plain. *Quat. Sci.* **1999**, *5*, 448–455.
12. Ren, C.Y.; Zhang, B.; Wang, Z.M.; Song, K.S.; Liu, D.W.; Liu, Z.M. A GIS-based Tupu analysis of dynamics of saline-alkali land in western Jilin province. *Chin. Geogr. Sci.* **2007**, *17*, 333–340.
13. Wang, Z.Q.; Zhang, B.; Yu, L.; Zhang, S.Q.; Wang, Z.M. Study on LUCC and the ecological security response of wetlands in western Jilin province. *Arid Zone Res.* **2004**, *21*, 97–103. (In Chinese)
14. Zang, L.J.; Jiang, Q.G.; Wang, F.Y. Adjustment of land utilization structure in Zhenlai County. *Glob. Geol.* **2010**, *29*, 149–154. (In Chinese)
15. Tang, J.; Wang, X.G. Analysis of the land use structure changes based on Lorenz curves. *Environ. Monit. Assess.* **2009**, *151*, 175–180.
16. Wang, Z.Q.; Zhang, B.; Zhang, S.Q.; Wang, Z.M. Study on dynamics of landscape and responses of ecological security to it in west Jilin province. *J. Soil Water Conserv.* **2005**, *19*, 131–136. (In Chinese)
17. Rogan, J.; Chen, D.M. Remote sensing technology for mapping and monitoring land-cover and land-use change. *Progr. Plan.* **2004**, *61*, 301–325.
18. Xiao, H.L.; Weng, Q.H. The impact of land use and land cover changes on land surface temperature in a karst area of China. *J. Environ. Manag.* **2007**, *85*, 245–257.
19. Coppin, P.; Jonckheere, I.; Nackaerts, K.; Muys, B.; Lambin, E. Digital change detection methods in ecosystem monitoring: A review. *Int. J. Remote Sens.* **2004**, *25*, 1565–1596.
20. Shafizadeh Moghadam, H.; Helbich, M. Spatiotemporal urbanization processes in the megacity of Mumbai, India: A Markov chains-cellular automata urban growth model. *Appl. Geogr.* **2013**, *40*, 140–149.
21. Deng, J.S.; Wang, K.; Li, J.; Deng, Y.H. Urban land use change detection using multisensory satellite images. *Pedosphere* **2009**, *19*, 96–103.
22. Weber, C.; Petropoulou, C.; Hirsch, J. Urban development in the Athens metropolitan area using remote sensing data with supervised analysis and GIS. *Int. J. Remote Sens.* **2005**, *26*, 785–796.
23. Deng, J.S.; Wang, K.; Hong, Y.; Qi, J.G. Spatio-temporal dynamics and evolution of land use change and landscape pattern in response to rapid urbanization. *Landsc. Urban Plan.* **2009**, *92*, 187–198.
24. Long, H.L.; Wu, X.Q.; Wang, W.J.; Dong, G.H. Analysis of urban-rural land-use change during 1995–2006 and its policy dimensional driving forces in Chongqing, China. *Sensors* **2008**, *8*, 681–699.
25. Dewan, A.M.; Yamaguchi, Y.; Rahman, M.Z. Dynamics of land use/cover changes and the analysis of landscape fragmentation in Dhaka Metropolitan, Bangladesh. *GeoJournal* **2012**, *77*, 315–330.
26. Buyantuyev, A.; Wu, J.G.; Gries, C. Multiscale analysis of the urbanization pattern of the Phoenix metropolitan landscape of USA: Time, space and thematic resolution. *Landsc. Urban Plan.* **2010**, *94*, 206–217.
27. Zhou, Q.M.; Li, B.L.; Kurban, A. Trajectory analysis of land cover change in arid environment of China. *Int. J. Remote Sens.* **2008**, *29*, 1093–1107.
28. Wang, D.C.; Gong, J.H.; Chen, L.D.; Zhang, L.H.; Song, Y.Q.; Yue, Y.J. Comparative analysis of land use/cover change trajectories and their driving forces in two small watersheds in the western Loess Plateau of China. *Int. J. Appl. Earth Obs. Geoinf.* **2013**, *21*, 241–252.
29. Mertens, B.; Lambin, E.F. Land-cover-change trajectories in southern Cameroon. *Ann. Assoc. Am. Geogr.* **2000**, *90*, 467–494.

30. Wang, D.C.; Gong, J.H.; Chen, L.D.; Zhang, L.H.; Song, Y.Q.; Yue, Y.J. Spatio-temporal pattern analysis of land use/cover change trajectories in Xihe watershed. *Int. J. Appl. Earth Obs. Geoinf.* **2012**, *14*, 12–21.
31. Zhou, Q.M.; Li, B.L.; Kurban, A. Spatial pattern analysis of land cover change trajectories in Tarim Basin, northwest China. *Int. J. Remote Sens.* **2008**, *29*, 5495–5509.
32. Swetnam, R.D. Rural land use in England and Wales between 1930 and 1998: Mapping trajectories of change with a high resolution spatio-temporal dataset. *Landsc. Urban Plan.* **2007**, *81*, 91–103.
33. Bai, S.Y.; Zhang, S.W. A study on the spatial-temporal land use conversion in county region—Taking Duerbete county as an example. *J. Arid Land Resour. Environ.* **2005**, *19*, 67–70. (In Chinese)
34. Zhao, B.; Kreuter, U.; Li, B.; Ma, Z.J.; Chen, J.K.; Nakagoshi, N. An ecosystem service value assessment of land-use change on Chongming Island, China. *Land Use Policy* **2004**, *21*, 139–148.
35. Isong, M.; Eyo, E.; Eyoh, A.; Nwanekezie, O.; Olayinka, D.N.; Udoudo, D.O.; Ofem, B. GIS cellular automata using artificial neural network for land use change simulation of Lagos, Nigeria. *J. Geogr. Geol.* **2012**, *4*, 94–101.
36. Lin, Y.P.; Chu, H.J.; Wu, C.F.; Verburg, P.H. Predictive ability of logistic regression, auto-logistic regression and neural network models in empirical land-use change modeling—A case study. *Int. J. Geogr. Inf. Sci.* **2011**, *25*, 65–87.
37. Lin, Z.M.; Xia, B.; Dong, W.J. Analysis on temporal-spatial changes of land-use structure in Guangdong province based on information entropy. *Trop. Geogr.* **2011**, *31*, 266–271. (In Chinese)
38. Henseler, M.; Wirsig, A.; Herrmann, S.; Krimly, T.; Dabbert, S. Modeling the impact of global change on regional agricultural land use through an activity-based non-linear programming approach. *Agric. Syst.* **2009**, *100*, 31–42.
39. Huang, Y.; Xia, B.; Yang, L. Relationship study on land use spatial distribution structure and energy-related carbon emission intensity in different land use types of Guangdong, China, 1996–2008. *Sci. World J.* **2013**, *2013*, Article ID 309680.
40. Zheng, X.Q.; Xia, T.; Yang, X.; Yuan, T.; Hu, Y.C. The land Gini coefficient and its application for land use structure analysis in China. *PLoS One* **2013**, *8*, e76165.
41. Ramankutty, N.; Foley, J.A. Estimating historical changes in global land cover: Croplands from 1700 to 1992. *Glob. Biogeochem. Cycles* **1999**, *13*, 997–1027.
42. Petit, C.C.; Lambin, E.F. Long-term land-cover changes in the Belgian Ardennes (1775–1929): Model-based reconstruction vs. Historical maps. *Glob. Chang. Biol.* **2002**, *8*, 616–630.
43. *Local Record of Zhenlai County*; Jilin People's Press: Changchun, China, 1995. (In Chinese)
44. Bai, S.Y.; Zhang, S.W. The discussion of the method of land utilization spatial information reappearance of history period. *J. Arid Land Resour. Environ.* **2004**, *18*, 77–80. (In Chinese)
45. Bai, S.Y.; Zhang, S.W.; Zhang, Y.Z. Study on the method of diagnose the plowland spacial distribution in historical era. *Syst. Sci. Comp. Stud. Agric.* **2005**, *21*, 252–255. (In Chinese)
46. Liu, J.Y.; Liu, M.L.; Zhuang, D.F.; Zhang, Z.X.; Deng, X.Z. Study on spatial pattern of land-use change in China during 1995–2000. *Science China* **2003**, *46*, 374–384.
47. Bai, S.Y.; Zhang, S.W.; Zhang, Y.Z. Stages and determinants of farmland development and driving forces in Duerbote County during the past 50 years. *Resour. Sci.* **2005**, *27*, 71–76. (In Chinese)
48. Lu, X.N.; Deng, W.; Zhang, S.Q.; Xong, D.H.; Xin, X. Land-use changes along the lower reaches of Huolin river in the last 50 years. *J. Arid Land Resour. Environ.* **2007**, *21*, 68–74. (In Chinese)

49. Liu, X.N.; Huang, F. Analysis of the regional co-environmental effect driving by LUCC. *J. Northeast Norm. Univ.* **2002**, *34*, 87–92. (In Chinese)
50. Song, K.S.; Liu, D.W.; Wang, Z.M.; Zhang, B.; Jin, C.; Li, F.; Liu, H.J. Land use change in Saijiang plain and its driving forces analysis since 1954. *Acta Geogr. Sinica* **2008**, *63*, 93–104. (In Chinese)
51. Wang, X.G.; Tang, J.; Li, Z.Y.; Wang, C.Y. Analysis of land use structure change in western of Jilin province based on Lorenze curves. *Res. Agric. Mod.* **2007**, *28*, 310–313. (In Chinese)

© 2014 by the authors; licensee MDPI, Basel, Switzerland. This article is an open access article distributed under the terms and conditions of the Creative Commons Attribution license (<http://creativecommons.org/licenses/by/4.0/>).